Designing Under Pressure

Andrew P.F. Little

Carl T.F. Ross

Daniel Short

Graham X. Brown

Little, Ross, Short and Brown introduce a new tool to better design pressure vessels.

Who should read this paper?

This paper will be of primary interest to structural designers involved in designing pressure vessels, particularly submarine structures. At present, there is very little 'non-military' information on designing deep-diving submarine pressure hulls.

Why is it important?

Under external pressure, pressure vessels can suffer catastrophic collapse. The purpose of the paper is to present easy-to-use design charts for use by structural designers who design pressure vessels. The design chart is innovative because it simplifies the design of complex structural failure modes, particularly those for deep-sea applications.

The oceans cover some 71% of the Earth's surface, but only about 0.1% of the oceans' bottoms have been explored. The charts will allow deep-diving submarines to be designed to greater advantage for commercial exploitation and for military purposes. The work described in this paper may ultimately improve our ability for retrieving deep-sea methane and for the burial of greenhouse gases, including carbon dioxide.

About the Authors

Andrew P.F. Little is the Principal Lecturer in Mechanical and Design Engineering at the University of Portsmouth, UK. His main expertise is in the statics and dynamics of submarine pressure hulls.

Carl T.F. Ross is a Professor of Structural Dynamics at the University of Portsmouth in the UK. He is an expert in statics and dynamics of submarine pressure hulls.

Daniel Short is a Mechanical Engineering student at the University of Portsmouth in the UK. His expertise is in the strength of submarine pressure hulls.

Graham X. Brown is the Chief Mechanical Engineer at Sonardyne Ltd., in Yately, Hampshire, UK. His expertise is in the research, design and construction of deep-sea pressure vessels.

INELASTIC BUCKLING OF GEOMETRICALLY IMPERFECT TUBES UNDER EXTERNAL HYDROSTATIC PRESSURE

ANDREW P.F. LITTLE[1], CARL T.F. ROSS[1], DANIEL SHORT[1] & GRAHAM X. BROWN[2]

1 Dept. of Mechanical & Design Engineering, University of Portsmouth, Portsmouth, United Kingdom.
2 Sonardyne International Ltd, Yateley, Hants. United Kingdom.

ABSTRACT

The paper reports on the buckling of 12 thin-walled geometrically imperfect tubes, which were tested to destruction under uniform external hydrostatic pressure. The paper also reports on other similar tests to destruction, carried out on quite a large number of geometrically imperfect tubes.

Theoretical studies were also carried out with well-known analytical solutions, together with a numerical solution using the famous finite element computer package, namely ANSYS.

Whereas the theoretical analyses agreed with each other, they did not agree with the experimental data for the shorter tubes; this was because the shorter tubes collapsed by inelastic instability due to initial geometrical imperfections of the tubes. Exact analysis of slightly geometrically imperfect tubes, with random distribution, has so far defied reliable theoretical solutions. However, this paper presents a design chart, which can cater to these geometrical imperfections. The design chart may also be suitable for large vessels such as submarines, off-shore drilling rigs, silos, etc.

KEYWORDS.
Geometrically imperfect tubes, initial out-of-roundness, inelastic buckling, external pressure, von Mises, finite elements, ANSYS.

NOMENCLATURE

A	mean shell radius
d	mean shell diameter
E	Young's modulus of elasticity
L	unsupported length of cylinder
L_0	overall length of a cylinder
n	number of circumferential lobes formed
P_{cr}	critical (theoretical) buckling pressure
P_{design}	design buckling pressure $= P_{pred} / SF$
P_{exp}	experimental buckling pressure
P_{pred}	predicted buckling pressure
PKD	Plastic Knockdown Factor
SF	Safety Factor
t	shell wall thickness
λ	Windenburg thinness ratio
υ	Poisson's ratio
σ_{yp}	yield stress

1. INTRODUCTION

Circular cylinders under external pressure often appear in the form of submarine pressure hulls, torpedoes, off-shore drilling rigs, silos, tunnels, immersed tubes, rockets, medical equipment, food cans, etc. Such vessels are good for resisting internal or external pressure, however under uniform external pressure they can collapse at a fraction of the pressure that will cause failure under internal pressure. Failure of these vessels under uniform external pressure is called non-symmetric bifurcation buckling or shell instability [1 to 3] and is shown in Figure. 1.

Figure 1: Shell instability.

Figure 2: Ring-stiffened circular cylinders.

To improve the resistance of these vessels to the effects of uniform external pressure, the vessels are usually stiffened by ring stiffeners spaced at near equal distances apart, as shown in Figure. 2.

If, however, the ring stiffeners are not strong enough, the entire flank of the vessel can collapse bodily by a mode called general instability and as shown in Figure 3 [3 to 7].

Figure 3: General instability.

Another mode of failure is known as axisymmetric deformation, where the cylinder implodes axisymmetrically, so that its cross-section keeps its circular form while collapsing, as shown in Figure 4.

Figure 4: Axisymmetric collapse.

In this study, we will be concerned with elastic and inelastic shell instability; as such vessels can collapse at pressures of a fraction of that to cause the vessels to fail under internal pressure. The resistance to external pressure is further worsened if the vessel suffers from initial out-of circularity. If the initial out-of-circularity is large and regular, such as that considered by Bosman et al [8], then analysis by non-linear numerical methods is satisfactory. If, however, the initial out-of-circularity is small and random, then exact or near exact theoretical analyses have so far been defied. Ross, however, has shown that such vessels can be analysed by his design chart of Figure 3.4 [3]. This design chart, however, was for near perfect vessels and is not suitable for vessels with small but significant initial geometrical imperfections, such as considered in the present paper. The process therefore is to calculate the theoretical buckling pressure for a perfect vessel by the von Mises formula [1 to 3], together with the Windenburg thinness ratio [2,3]. Then, using the thinness ratio, a plastic knockdown factor (PKD) can be determined from the design chart and divided into the theoretical von Mises buckling pressure to give the predicted buckling pressure, where.

P_{cr} = theoretical von Mises elastic buckling pressure.
λ = Windenburg thinness ratio.

P_{pred} = Predicted buckling pressure = P_{cr}/PKD.
P_{design} = P_{pred}/SF
SF = a safety factor.
i.e. $P_{design}=P_{cr}/(PKD*SF)$

1.1. VON MISES BUCKLING PRESSURE

This states that the elastic instability pressure for a thin walled circular cylindrical shell simply supported at both ends and subjected to combined actions of uniform lateral and axial pressure [1 to 3] is given by equation (1).

$$P_{cr} = \frac{E(t/a)}{\left[n^2 - 1 + 0.5(\pi a/l)^2\right]} \times \left\{ \frac{1}{\left[n^2(l/\pi a)^2 + 1\right]^2} + \frac{t^2}{12a^2(1-v)^2}\left[n^2 - 1 + \left(\frac{\pi a}{l}\right)^2\right]^2 \right\} \quad (1)$$

Where,

P_{cr} = buckling pressure;
t = wall thickness of circular cylinder;
a = mean radius of circular cylindrical shell;
/ = unsupported length of cylinder;
E = Young's Modulus;
v = Poisson's ratio;
n = No. of circumferential lobes.

1.2. WINDENBURG AND TRILLING'S BUCKLING PRESSURE

Windenburg and Trilling's paper states the buckling equation for a long, thin, perfectly circular cylinder, under uniform external pressure, is given by equation (2). This formula is also known as the David Taylor Model Basin (DTMB) [3].

$$P_{cr} = \frac{2.42E(t/2a)^{5/2}}{\left(1-v^2\right)^{0.75}\left[(l/2a) - 0.447(t/2a)^{1/2}\right]} \quad (2)$$

Where,

P_{cr} = buckling pressure;
t = wall thickness of circular cylinder;
a = mean radius of circular cylindrical shell;
E = Young's Modulus;
v = Poisson's ratio.

The predicted pressure P_{cr} used in this paper is that of von Mises.

P_{cr1} = von Mises calculations for the 2006 investigation
P_{cr3} = von Mises calculations for the current investigation.

1.3 WINDENBURG AND TRILLING'S THINNESS RATIO λ

Windenburg and Trilling obtained their thinness ratio [1-3] by the following approach:

They noted that experimental tests on short circular section tubes under external hydrostatic pressure had found that they fail when their circumferential stress reaches yield, according to the well-known Boiler formula [3,6], as follows.

σ_{yp} = pd/(2t)
or $p=\sigma_{yp}*(2t)/d$, (3)
where p= pressure to cause yield.
d= 2a
σ_{yp} =Yield Stress

They further noted that experiments had shown that when long thin-walled circular tubes are subjected to external hydrostatic pressure, they can buckle elastically according to the von Mises or the DTMB formula of equations (1) & (2). Experiments on circular section tubes of intermediate and shorter lengths, when a thinness ratio, namely λ[2,3], has a value of less than 0.4, have shown that they fail somewhere in-between the pressures of equations (1) and (3). Windenburg and Trilling [2, 3] argued that if we equated equations (2) and (3), we can get a thinness ratio relating these two modes of failure, which will enable us to precisely predict the collapse pressures for intermediate circular cylinders; they called this their thinness ratio 'λ.' Now if we examine equation (2), we can see that in the denominator on the right hand side of equation (2), that //d is much larger than $0.45*(t/d)^{0.5}$, thus if we neglect $0.45*(t/d)^{0.5}$ and assume that v = 0.3, we can simplify equation (2) to the form:

$$P_{cr} = 2.6*E*(t/d)^{2.5}/(l/d) \quad (4)$$

Equating (3) and (4), we get $\sigma_{yp}*(2t) / d = 2.6E*(t/d)^{2.5} / (l/d)$,
Or $\sigma_{yp}*t/d = \lambda^2 * E*(t/d)^{2.5} / (l/d)$,
Or $\lambda^2=(l/d) / (t/d)^{-1.5} * (\sigma_{yp} / E)$
Or $\lambda= [(l/d)^2 / (t/d)^3]^{0.25} * (\sigma_{yp} / E)^{0.5}$

N.B. Windenburg and Trilling squared λ in the above calculation, so that for most intermediate length vessels, the value of λ would be approximately one.

2. EXPERIMENTAL TESTING

In order to obtain the required chart to enable the theoretical predictions to be made, experimental work had to be preformed. This was done by using a high-pressure test tank (see Figure 5). Specimens were tested to destruction and the failure pressures recorded.

Figure 5: Pressure Test Rig.

Test Equipment:

- High-Pressure Vessel
- Hydraulic Pump
- Pressure Gauge

2.1 THE TESTING PROCEDURE

The pressure pump was a hand-operated hydraulic one that could exert a maximum pressure of 6,000 psi (414 bar), and as it was hand operated, line losses were negligible. Additionally, as it was hand-operated, the applied pressure could be increased in increments of about 1psi (0.07 bar); thus, the experimental buckling pressures were precisely determined. The tank was capable of sustaining a pressure of 3,000 psi (207 bar).

The closure discs were push-fitted into the ends of each specimen to seal each specimen and to make it watertight. A photograph of the end bungs is shown in Figures 6 to 8. The specimen was then placed into the pressure tank, just resting in the tank itself and unattached to it. That is, the boundary conditions for each specimen were assumed to be simply-supported between the 'O' rings in the closure discs. The ends of the specimen were free to rotate during the collapse of each specimen.

The tank lid was fitted and screwed down firmly.

The bleed valve at the top of the tank was opened and the trapped air expelled from the tank by gently pumping in water.

After the trapped air was expelled, the bleed valve was sealed to make the system pressure-tight.

The hydraulic pressure in the tank was increased via the hydraulic pump in small increments.

The pressure gauge was carefully monitored until failure occurred. Failure occurred with a bang which could easily be heard, together with a large fall in pressure.

The collapse pressure was recorded and the pressure drop noted, as well.

The hydraulic pressure was released and then the tank lid was removed to retrieve and examine the collapsed specimen.

Figure 6: The end bungs or closure discs.

Figure 7: Some of Nagoppan's models, with end bungs.

2.2. THE TEST SPECIMENS

The test specimens used for this experiment were aluminum alloy tubes. The tubes were supplied by Sonardyne for research into the buckling effect of Aluminum 6082-T6 seamless tubes. The two supplied tubes came in lengths, which were machined to the desired lengths for each test specimens, Figure 8; their details were as follows:

Figure 8: Test Specimens and End Caps.

- Outer Diameter = 50mm
- Wall Thickness = 1.7mm
- Young's Modulus = 70,000 MPa
- Poisson's Ratio = 0.3
- Yield Stress = 250 MPa
- Density = 2,620 kg/m^3

The two mild steel end caps were machined for push fit connections into the tube ends; these can be seen in Figures 6 to 8. Sealing was achieved by the use of a size As568A-233 O-ring, manufactured in 'Nitrile'.

3. ANALYSES

3.1 USING MISESNP FOR THE RESULTS OF NAGOPPAN [9]

Using the computer program MisesNP [3] the vessels of Nagoppan [9] were first analysed; the results are reproduced here because this data will be used to produce a more heavily populated design chart in the present paper than that provided by Nagoppan. It is necessary to produce a more heavily populated design chart, because many such vessels collapse at lower or higher buckling pressures than expected. Such vessels are said to give haphazard or rogue results.

MisesNP [3] is a DOS based program devised to calculate the shell instability buckling pressures of cylinders; the program was written by Ross [3]. MisesNP uses the von Mises formula [1], together with the formula of Windenburg and Trilling's [2]) to calculate the buckling pressures of circular cylinders under uniform external pressure, together with their thinness ratios; these were for an isotropic material (see Table 1).

When using MisesNP the following parameters had to be inputted:

1. Unsupported Length in mm = L
2. Mean Radius in mm
3. Wall Thickness in mm
4. Young's Modulus in MPa
5. Poisson's Ratio
6. Yield Stress in MPa

Model	Length	Lambda		P_{cr1} von Mises		P_{cr1} DTMB
	L (m)	λ	1/λ	Lobes	Pressure (MPa)	Pressure MPa
tube1	0.378	2.058	0.486	2	6.96	5.45
tube2	0.378	2.058	0.486	2	6.96	5.45
tube3	0.378	2.058	0.486	2	6.96	5.45
tube4	0.315	1.879	0.532	2	7.20	6.55
tube5	0.315	1.879	0.532	2	7.20	6.55
tube6	0.315	1.879	0.532	2	7.20	6.55
tube7	0.252	1.681	0.595	2	7.77	8.22
tube8	0.252	1.681	0.595	2	7.77	8.22
tube9	0.252	1.681	0.595	2	7.77	8.22
tube10	0.189	1.456	0.687	2	9.62	11.01
tube11	0.189	1.456	0.687	2	9.62	11.01
tube12	0.189	1.456	0.687	2	9.62	11.01
tube13	0.126	1.188	0.842	2	18.65	16.71
tube14	0.126	1.188	0.842	2	18.65	16.71
tube15	0.126	1.188	0.842	2	18.65	16.71
tube16	0.063	0.840	1.190	3	33.69	34.57
tube17	0.063	0.840	1.190	3	33.69	34.57
tube18	0.063	0.840	1.190	3	33.69	34.57

Table 1: MisesNP results for calculating properties.

3.2. PLASTIC KNOCKDOWN FACTOR (PKD)

Knowing the experimental buckling pressures for Tubes 7 to 18, the PKDs were determined for these tubes, as shown in Table 2. Theoretical calculations using Windenburg and Trilling's formulae gave us the buckling pressure Pcr and thinness ratios ( ). The experimental buckling pressure for the cylinders were denoted by the symbol Pexp. From these results, it was possible to calculate the plastic knockdown factor, namely (PKD) [3], where:

$PKD = P_{cr}/P_{exp}$

Note:

Experimental work not carried out in the 2006 investigation was represented by the symbol (-); this was because of the height of the pressure tank wasn't long enough for some of the models.

To generate a design chart, the calculated PKD was plotted against 1/λ this was successfully achieved by Ross [3]; but his design chart could not cope with shorter and thicker models.

3.3. USING ANSYS

ANSYS is a finite element software package that addresses many problems in engineering science, but especially problems in structural mechanics. It also provides nonlinear [8] capabilities and complex finite elements, together with inelastic material models. This aids the designer to simulate an accurate prediction of how a structure behaves when a load has been applied. For every simulation that is performed, certain parameters have to be set, as follows:

- Model dimensions; unsupported length, mean radius and wall thickness;
- Material properties i.e. Young's modulus, Poisson's ratio and density;
- Boundary conditions; these were assumed to be simply-supported, similar to Portsmouth's in-house program namely 'MisesNP;'
- Structural conditions, which were 'Eigen buckling' in this case.

3.3.1 ANSYS SHELL 93 METHODOLOGY

Shell 93 is an eight node isoparametric 'rectangular' element; it is a very popular and a well-tried and reliable element. A brief description of how each vessel was analysed is as follows:

1. Model dimensions and properties

The first step was to create a solid cylinder using the model's dimensions. Once this was entered, the model

Table 2: Results for calculating PKD

Model	Length	Lambda				PKD	P_{exp}
	L M	Λ	1/λ	Lobes (n)	Pressure MPa		2006 MPa
tube1	0.378	2.058	0.486	2	6.96	-	-
tube2	0.378	2.058	0.486	2	6.96	-	-
tube3	0.378	2.058	0.486	2	6.96	-	-
tube4	0.315	1.879	0.532	2	7.20	-	-
tube5	0.315	1.879	0.532	2	7.20	-	-
tube6	0.315	1.879	0.532	2	7.20	-	-
tube7	0.252	1.681	0.595	2	7.77	0.909	8.552
tube8	0.252	1.681	0.595	2	7.77	1.043	7.448
tube9	0.252	1.681	0.595	2	7.77	1.024	7.586
tube10	0.189	1.456	0.687	2	9.62	0.955	10.069
tube11	0.189	1.456	0.687	2	9.62	1.395	6.897
tube12	0.189	1.456	0.687	2	9.62	0.955	10.069
tube13	0.126	1.188	0.842	2	18.65	1.536	12.138
tube14	0.126	1.188	0.842	2	18.65	1.470	12.690
tube15	0.126	1.188	0.842	2	18.65	1.486	12.552
tube16	0.063	0.840	1.190	3	33.69	2.181	15.448
tube17	0.063	0.840	1.190	3	33.69	2.181	15.448
tube18	0.063	0.840	1.190	3	33.69	2.181	15.448

now had to be converted into a tube. Using the element type command, the Shell 93 8-node element was selected; this converted the solid cylinder into a tube and the material properties were then applied.

2. Meshing

Once the tube had been generated, it was possible to increase the precision of the analysis by using the mesh tool command, namely 'automesh'. One can define how many elements one would like to analyse and for this investigation all analyses had an average of about 1,000 elements. To judge the precision of this procedure, several of the tubes were analysed with less than half this number of elements and the difference in buckling pressures predicted when using about 1,000 elements compared with less than about 500 elements was less than 1%. Thus, it was decided that all models could be auto-meshed with about 1,000 elements.

3. The boundary conditions

These relate to how the tube was constrained and how the loading was applied. For this investigation the left hand side of the tubes was constrained along all three 'translational' axes, namely X, Y and Z and the right hand side was constrained along the 'translational' X and Y directions only; this enabled the tube to move along the Z axis (axially) and to rotate about both ends. Thus, the boundary conditions represented simply-supported ends and it was believed that this combination of constraints best represented the effects of the end caps (see Figure 9).

4. Structural analysis

For the structural analysis a pre-stress of –1MPa was applied on the outer surface of the cylinder, the value of –1MPa was theoretical and represented a 'pre-stress' external pressure. The next stage was to apply a pre-stress option and to perform a static analysis.

5. Eigen buckling

After the static analysis was carried out, the buckling analysis could be done. This called for a 'new analysis' to be performed using the 'Eigen buckling' option. The buckling mode was set to 5 using the 'Block Lanczos' and the load step option set to the same mode value of 5; this would give the 5 lowest buckling pressures.

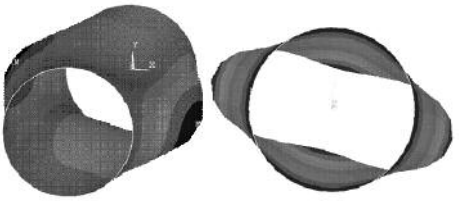

Figure 10: Buckling of a 189 mm tube.

6. Results

Using the 'result summary' command, it was possible to read the buckling pressure for the first five buckling modes, the lowest of these was recorded and tabulated in Table 3. Additionally it was possible to run the simulation property by using the 'animate' command. Figure 10 shows a snap shot of the buckling mode of a typical cylindrical tube.

The required buckling pressure was the lowest of the 5 values generated for each vessel and the value of 'n', the number of lobes that the vessel buckled into; this was obtained by graphically plotting the eigenmode, corresponding to the appropriate value of buckling pressure on the screen; i.e. 'n' was counted. The buckling pressures could be obtained either from a table or from the graphical plot of the eigenmode, which was plotted on the screen; where it was referred as a 'frequency' value.

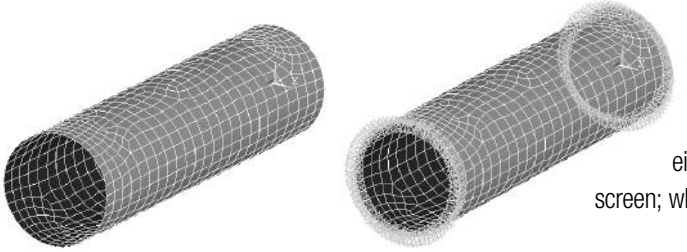

Figure 9: The mesh and the boundary conditions that were applied to the cylinder.

Model	Unsupported Length L (m)	lambda		P_{cr1} Ansys Shell 93	
		λ	1/λ	lobes (n)	pressure (MPa)
tube1	0.378	2.058	0.486	2	9.80
tube2	0.378	2.058	0.486	2	9.80
tube3	0.378	2.058	0.486	2	9.80
tube4	0.315	1.879	0.532	2	10.36
tube5	0.315	1.879	0.532	2	10.36
tube6	0.315	1.879	0.532	2	10.36
tube7	0.252	1.681	0.595	2	11.73
tube8	0.252	1.681	0.595	2	11.73
tube9	0.252	1.681	0.595	2	11.73
tube10	0.189	1.456	0.595	2	16.45
tube11	0.189	1.456	0.687	2	16.45
tube12	0.189	1.456	0.687	2	16.45
tube13	0.126	1.188	0.842	2	24.08
tube14	0.126	1.188	0.842	2	24.08
tube15	0.126	1.188	0.842	2	24.08
tube16	0.063	0.840	1.190	3	48.45
tube17	0.063	0.840	1.190	3	48.45
tube18	0.063	0.840	1.190	3	48.45

Table 3: Ansys Shell 93 Results for Aluminium 6082-T-6 seamless tubes.

3.4 NAGOPPAN'S RESULTS

Naggopan's results [9] appeared to be very successful, but they were sparse for shorter and thicker tubes and because of this they were not completely reliable; it was because of this that the current work was carried out. As many such vessels collapse at unexpectedly higher or lower pressures than predicted, it was necessary to obtain a more densely populated design chart. A photograph of one of Nagoppan's buckled models, together with an end bung, is shown in Figure 11.

3.5 THE CURRENT WORK

3.5.1 JUSTIFICATION FOR TUBE LENGTH SELECTION

Nagoppan's design chart was sparsely populated in the PKD regions of 0.1 to 1.0 and from 0.8 to 3 and as many large vessels will fall into this region, it was necessary to extend his design chart. Thus, in order to more sensibly populate the chart and continue the study, it was decided to select tube lengths for further testing that would enable more population of the sparse areas, thereby improving the uniformity of the graphic display.

Figure 11: A closure disc with a buckled specimen.

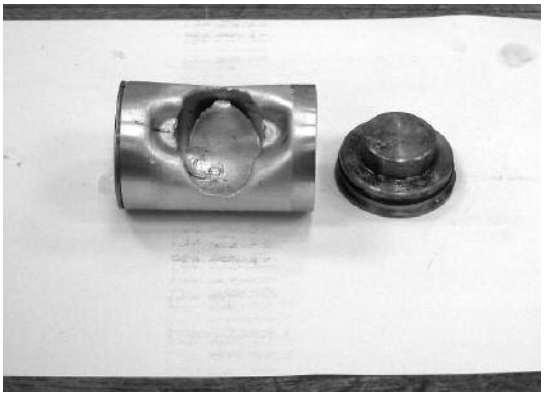

length mm	PKD
230	1
160	1.5
103	2
83	3
63	4
50	4
30	5

Table 4.

3.5.2 TUBE LENGTHS

Tube lengths were chosen to correspond to their predicted PKD values (see Table 4).

A tolerance of 0.05mm on the length of each tube was used; this was adequate for parting off on a standard lathe and it amounted to a tolerance for the shortest tubes of about 0.17% and for the longest tubes of about 0.02%. The effects of these length tolerances were negligible on the effects of the results and the theoretical predictions.

3.6 METEOROLOGY

To gain an accurate representation of the geometry of the tubes, they were measured using a Computer Controlled Measuring (CMM) machine. A 63mm Specimen was sent to Solent Mould Tools Ltd. in Waterlooville, HANTS to be measured. They took points around the circumference of the tube at 4 locations (see Figure 12 for the results of a cross-section of the tubing).

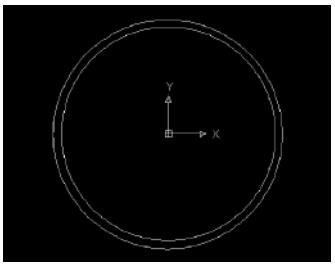

Figure 12: Cross section of tubing.

A 230mm long specimen was sent to the metrology laboratory at the University of Portsmouth. The aim of the measuring process was to see what the profile of the tube looked like, internal and externally. 100 Points were taken around the circumference in two areas 1) Z -5.0mm, 2) Z -224.99mm. Then the resulting data was plotted on to a graph, which magnified the profile.

The resulting data confirmed that the tubes were eccentric and that their profiles were consistently similar throughout (see Table 5). The reason for this was because the aluminium was drawn through a die; if the die were not positioned correctly, the tube would have had the same fault through its length. For the purposes of this study, we had to accept that all specimens had similar cross-sections throughout.

	External		Internal	
	Z-5.0mm	Z-224.9mm	Z-5.0mm	Z-224.9mm
No. of Points	100	100	100	100
Variance (mm)	0.0416	0.0423	0.0465	0.047
Circularity (mm)	0.155	0.1578	0.1893	0.1902
Diameter (mm)	50.805	50.806	47.514	47.516

Table 5: CMM results data for the 230 mm tube.

3.7 EXPERIMENTAL RESULTS

The experimental results are given in Table 6.

3.8 FAILURE MODES

Ross states in his book [3], that under uniform external pressure, a thin-walled circular cylinder may buckle in the manner shown in Figure 1; usually at a fraction of that pressure required causing axisymmetric yield. If the cylinder is very long, its buckling resistance will be very small, the vessel suffering failure in a flattening mode (i.e. ovalling), as shown in Figure 13.

From experimental results carried out in the 2006 investigation and in the present paper, it was clear that

Figure 13: Ovalling of cylinder.

this was true. All cylinders over 189mm failed in this manner, at a lower pressure than that predicted by the von Mises and Windenburg and Trilling's calculations (see Table 6).

Figure 14 shows the cross-sections of the theoretical circumferential wave patterns of the buckling modes due to elastic instability, under external pressure and Figures 15 & 16 show the collapsed vessels.

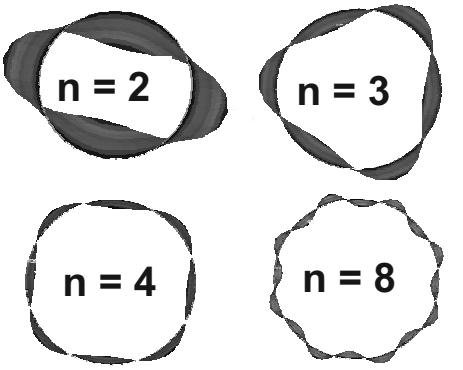

Figure 14: Circumferential wave patterns for buckling modes.

Model	Overall Length L_o	Unsupported Length L	P_{exp}	P_{exp}	P_{exp}	Fell to	Fell to	Fell to	Observation after Failure	Date
	m	m	MPa	bar	psi	MPa	bar	psi		
Tube 1	0.230	0.211	10.00	100.00	1450	1.59	15.9	230	elastic instability, resistance small (ovalling)	03/04/2007
Tube 2	0.160	0.141	12.96	129.60	1880	2.34	23.4	340	Inelastic instability due to initial geometrical imperfections	03/04/2007
Tube 3	0.160	0.141	14.34	143.40	2080	2.07	20.7	300	Inelastic instability due to initial geometrical imperfections	03/04/2007
Tube 4	0.103	0.084	15.86	158.60	2300	0.97	9.7	140	Inelastic instability due to initial geometrical imperfections	03/04/2007
Tube 5	0.103	0.084	16.82	168.20	2440	0.97	9.7	140	Inelastic instability due to initial geometrical imperfections	03/04/2007
Tube 6	0.103	0.084	15.86	158.60	2300	4.14	41.4	600	Inelastic instability due to initial geometrical imperfections	04/04/2007
Tube 7	0.083	0.064	17.37	173.70	2520	0.69	6.9	100	Inelastic instability rupturing 90° 41.5mm from end	04/04/2007
Tube 8	0.083	0.064	17.24	172.40	2500	0.83	8.3	120	Inelastic instability rupturing 90° 41.5mm from end	04/04/2007
Tube 9	0.083	0.064	16.41	164.10	2380	0.83	8.3	120	Inelastic instability rupturing 90° 41.5mm from end	04/04/2007
Tube 10	0.063	0.044	20.13	201.30	2920	1.93	19.3	280	Rupturing 90° along the edge of the bung with crack 180° to bung bent inwards	04/04/2007
Tube 11	0.063	0.044	19.31	193.10	2800	1.38	13.8	200	Rupturing 90° along the edge of the bung with crack 180° to bung bent inwards	04/04/2007
Tube 12	0.063	0.044	19.44	194.40	2820	1.24	12.4	180	Rupturing 90° along both edge of the bung with crack 180° to bung bent inwards	04/04/2007
Tube 13	0.050	0.031	-	-	-	-	-	-	crack properation through supported end (destoyed)	-
Tube 14	0.050	0.031	-	-	-	-	-	-	-	-
Tube 15	0.050	0.031	-	-	-	-	-	-	-	-
Tube 16	0.030	0.011	-	-	-	-	-	-	-	-
Tube 17	0.030	0.011	-	-	-	-	-	-	-	-
Tube 18	0.030	0.011	-	-	-	-	-	-	-	-

Table 6: Experimental Results.

3.9 PICTORIAL RESULTS OF EXPERIMENTS CARRIED OUT IN 2007

Figure 15: Picture of all specimens that were tested in 2007.

Models 2-3: Length 160mm, buckled due to inelastic shell instability.

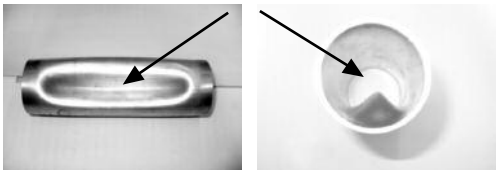

Models 7-9: Length 83mm, buckled due to inelastic shell instability; all rupturing.

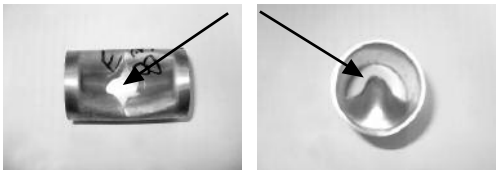

Models 10-12: Length 63mm, all ruptured.

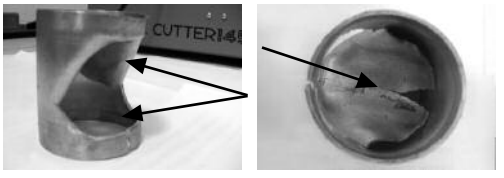

Figure 16: The collapsed vessels.

3.10 USING MISESNP

When using MisesNP (Figure 17) certain parameters had to be set for this analysis; these were described in Section 3. A screen shot when using 'MisesNP' is shown in Figure 17.

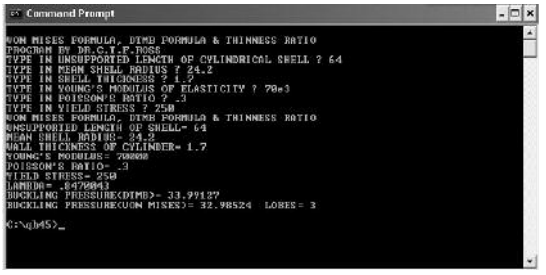

Figure 17: Screen shot of 'MisesNP' when calculating Pcr3 for a Model Tube.

3.11. PLASTIC KNOCKDOWN FACTOR FOR THE PRESENT SERIES

Theoretical calculations using Windenburg and Trilling's theorem produced the buckling pressures Pcr, together with the thinness ratios ( ). Experimental results gave values for the buckling pressure for the cylinders, namely P_{exp}. From these results, it was possible to calculate the plastic knockdown factor, namely PKD [3]; see Table 7, where

$$PKD = P_{cr}/P_{exp}$$

Note:

The symbol (-) represents missing data that was not carried out during the experiments of 2007; this was due to the maximum pressure constraints of the pressure tank.

3.12. USING ANSYS SHELL 93

ANSYS predictions were carried out for each of the specimen lengths, so that direct comparison could be made to the other prediction methods, the results of the analysis are tabulated in Table 8.

The following parameters had to be fed in:

- Model dimensions; unsupported length, mean radius and wall thickness;
- Material properties i.e. Young's modulus, Poisson's ratio and Density;
- Boundary conditions;
- Structural conditions (i.e. Eigen buckling).

Model	length	lambda		P_{cr3} von Mises				P_{cr3} DTMB	PKD	P_{exp}	P_{exp}
	L	λ	1/λ	Lobes	Pressure	Pressure	Pressure	Pressure		2007	2007
	m				MPa	bar	Psi	MPa		MPa	Psi
Tube 1	0.211	1.538	0.650	2	8.69	86.9	1260	9.84	0.869	10.00	1450
Tube 2	0.141	1.257	0.800	2	14.83	148.3	2150	14.88	1.144	12.96	1880
Tube 3	0.141	1.257	0.800	2	14.83	148.3	2150	14.88	1.034	14.34	2080
Tube 4	0.084	0.970	1.031	3	24.62	246.2	3570	25.48	1.552	15.86	2300
Tube 5	0.084	0.970	1.031	3	24.62	246.2	3570	25.48	1.464	16.82	2440
Tube 6	0.084	0.970	1,.031	3	24.62	246.2	3570	25.48	1.552	15.86	2300
Tube 7	0.064	0.847	1.181	3	32.99	329.8	4784	33.99	1.899	17.37	2520
Tube 8	0.064	0.847	1.181	3	32.99	329.9	4784	33.99	1.914	17.24	2500
Tube 9	0.064	0.847	1.181	3	32.99	329.9	4784	33.99	2.010	16.41	2380
Tube 10	0.044	0.702	1.425	4	50.96	509.6	7389	51.02	2.532	20.13	2920
Tube 11	0.044	0.702	1.425	4	50.96	509.6	7389	51.02	2.639	19.31	2800
Tube 12	0.044	0.702	1.425	4	50.96	509.6	7389	51.02	2.621	19.44	2820
Tube 13	0.031	0.589	1.700	4	74.88	748.8	10858	75.66	-	-	-
Tube 14	0.031	0.589	1.700	4	74.88	748.8	10858	75.66	-	-	-
Tube 15	0.031	0.589	1.700	4	74.88	748.8	10858	75.66	-	-	-
Tube 16	0.011	0.351	2.849	5	283.28	2832.8	41076	294.4	-	-	-
Tube 17	0.011	0.351	2.849	5	283.28	2832.8	41076	294.4	-	-	-
Tube 18	0.011	0.351	2.849	5	283.28	2832.8	41076	294.4	-	-	-

Table 7: Results for calculating PKD

3.13 USING PRO ENGINEER'S 'MECHANICA'

One part of the project was to carry out a feasibility study of a plastic buckling analysis by ANSYS of a tube that was eccentric about its longitudinal axis. Although ANSYS was capable of analysing such a vessel, its geometric modeller was not as good as that of Pro Engineer. However, although Pro Engineer's geometric modeller was very good, its finite element capabilities did not allow plastic buckling and were therefore not as good as ANSYS. However, Pro Engineer's model could be imported into ANSYS and also Pro Engineer's Mechanica was capable of statically analysing a tube that was eccentric about its longitudinal axis. For these reasons it was decided to geometrically model the eccentric tube in Pro Engineer and then import this model into ANSYS to carry out a feasibility study to see if a plastic buckling analysis of an eccentric tube could be carried by ANSYS. Also to see the static stress distribution for a tube that was eccentric about its longitudinal axis. From the CMM data obtained from Solent Mould Tools, two three-dimensional models were generated.

3.13.1 MODEL 1: ECCENTRIC TUBE

Using the X and Y co-ordinates, a consistent eccentric tube was generated. Then a uniform pressure was applied to its exterior surface using Mechanica. The pressure value was that of Pcr3 for model 4 (see Figure 18).

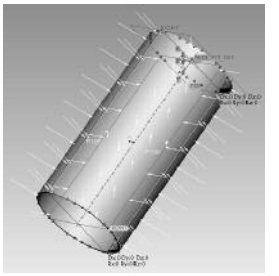

Figure 18: Eccentric tube with pressure loading.

Results from Mechanica showed a maximum stress of 450MPa was acting at both ends of the tube, together with a maximum displacement of 0.17mm (see Figure 19); this 'tied in' with the positions of experimental failure of the tubes and showed that Mechanica was of use for this analysis.

Model	Unsupported	lambda		P_{cr3} Ansys 93	
	L (m)	λ_3	$1/\lambda_3$	lobes (n)	pressure (MPa)
Tube 1	0.211	1.538	0.650	2	14.16
Tube 2	0.141	1.257	0.800	3	23.13
Tube 3	0.141	1.257	0.800	3	23.13
Tube 4	0.084	0.970	1.031	3	32.1
Tube 5	0.084	0.970	1.031	3	32.1
Tube 6	0.084	0.970	1.031	3	32.1
Tube 7	0.064	0.847	1.181	3	47.52
Tube 8	0.064	0.847	1.181	3	47.52
Tube 9	0.064	0.847	1.181	3	47.52
Tube 10	0.044	0.702	1.425	4	60.66
Tube 11	0.044	0.702	1.425	4	60.66
Tube 12	0.044	0.702	1.425	4	60.66
Tube 13	0.031	0.589	1.700	5	89.9
Tube 14	0.031	0.589	1.700	5	89.9
Tube 15	0.031	0.589	1.700	5	89.9
Tube 16	0.011	0.351	2.849	8	681.3
Tube 17	0.011	0.351	2.849	8	681.3
Tube 18	0.011	0.351	2.849	8	681.3

Table 8: ANSYS Shell 93 Results for Aluminium 6082-T-6 seamless tubes.

3.13.2 MODEL 2: ECCENTRIC TUBE

The CMM data acquired from Solent Mould Tools produced a three dimensional representation of the 63mm tube. During the measuring process the CMM machine took points around the circumference at 4 points.

Using Pro Engineer, these points were generated using the co-ordinate

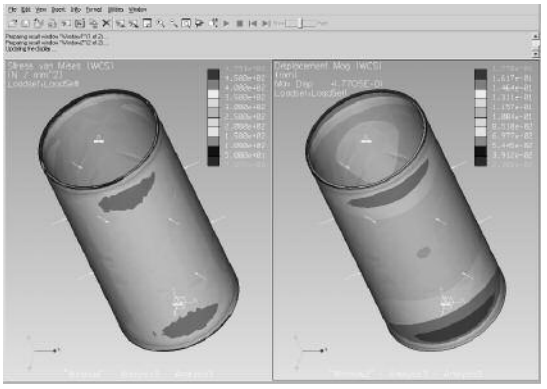

Figure 19: Screen Shot From Mechanica showing the maximum Von Mises stress and displacement.

references that were provided. Then using the sweep command the rings were joined together (see Figure 20).

A uniform pressure was applied to the exterior of the cylinder using Pro Engineer's Mechanica. The pressure value was that of Pcr3 for model 4 (see Figure 21).

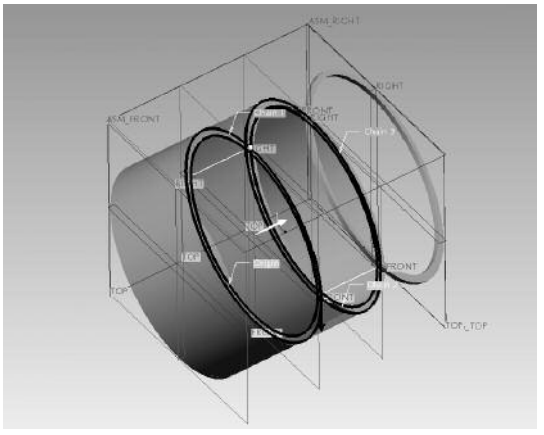

Figure 20: Screen shot of sweep.

Results from the Mechanica analysis clearly showed the significant areas of stress concentration and maximum displacement (see Figure 22). From studying the deformed test pieces, this was 'exactly' where each tube failed due to inelastic shell instability. Unfortunately, Mechanica can only perform static pressure loading and not plastic buckling. Nevertheless, the present study showed that Pro Engineer could be imported into ANSYS and a separate study (not reported here) showed that ANSYS could carry out a successful plastic buckling analysis of an eccentric tube under uniform external pressure. The purpose of the present study, however, was to provide an alternative but simpler method of predicting the plastic buckling pressure of slightly geometrically imperfect tubes. In any case, the above 'Pro Engineer/ANSYS' analysis would not be of much use for the design of a large vessel, such as a submarine pressure hull, as metrological measurements would be required prior to its manufacture, which is impossible. This emphasises the need for the design chart approach adopted in the present paper, where the maximum permissible out-of-roundness for a full-scale vessel, such as a submarine pressure hull, can be given to the constructors of the vessel, prior to its manufacture.

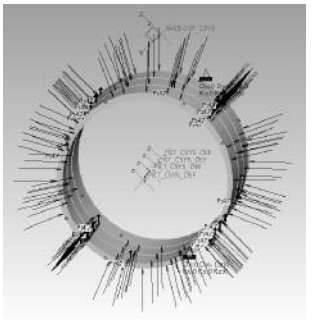

Figure 21: Pressure loading

4. DESIGN CHART

Once all the theoretical and experimental results had been calculated, it was possible to generate a design chart. This was done by plotting $1/\lambda$ against PKD. Figure 23 shows the design chart for Aluminum 6082-T6 seamless tubes form data obtained from experiments carried out in 2006 and 2007, together with those of References [2 and 7], which used other metals. Initial

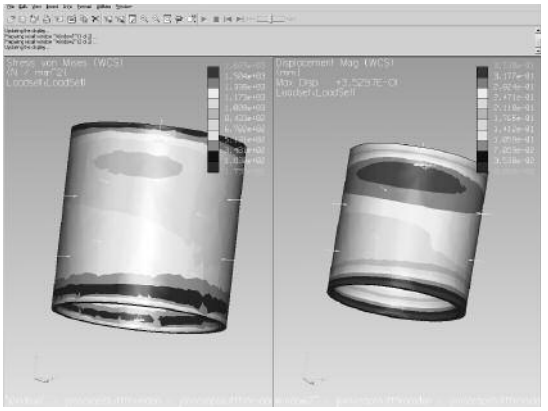

Figure 22: Screen Shot From Mechanica showing maximum von Mises stress and displacement.

imperfections of the aluminium alloy tubes of the present paper were between 0.104t to 0.13t, where 't' was the wall thickness of the vessels, and the corresponding values for those of Windenburg and Trilling were between 0.11t & 0.16t, where 't' was the wall thickness of their vessels.

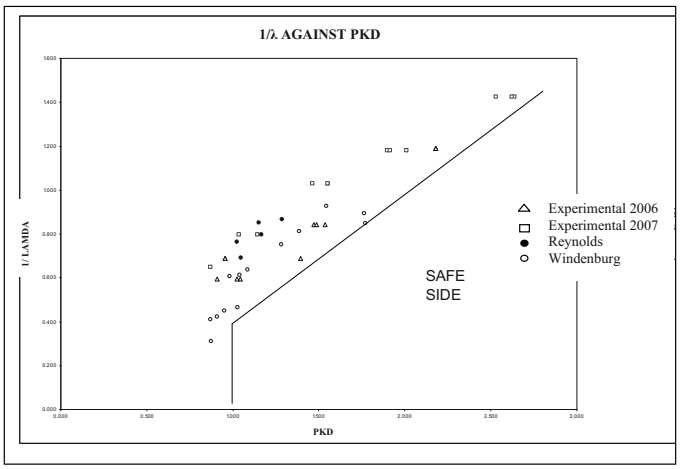

Figure 23: Updated Design Chart.

This design chart can now be used to calculate the predicted (experimental) buckling pressure Ppred for a pressure vessel made out of a similar material. During the process of obtaining the design charts, the factors PKD and had to be calculated. Now, as we have a design chart, it is possible to obtain the PKD from the Design Chart (Figure 23), which then can be used to calculate the predicted buckling pressure, namely Ppred [3]; where

$$P_{pred} = \frac{P_{cr}}{PKD}$$

4.1 DESIGN CHARTS & COMPARISONS

The graph of Figure 24 compares the theories of von Mises, Windenburg and Trilling, ANSYS Shell 93 and Experimental results obtained from the present study. It is evident from this graph that the prediction models, like those of 2006 [9], results in much higher predicted buckling pressures than the experimental results, especially for the shorter vessels. The results for Pro Engineer's 'Mechanica' are not shown, as it was not intended to use Mechanica for buckling analysis.

Results from experimental data acquired in 2006 - 2007 and ANSYS Shell 93 have been plotted in Figure 25 (1/λ against PKD), where in Figure 25:

PKD = $P_{cr(ANSYS)}/P_{exp}$.

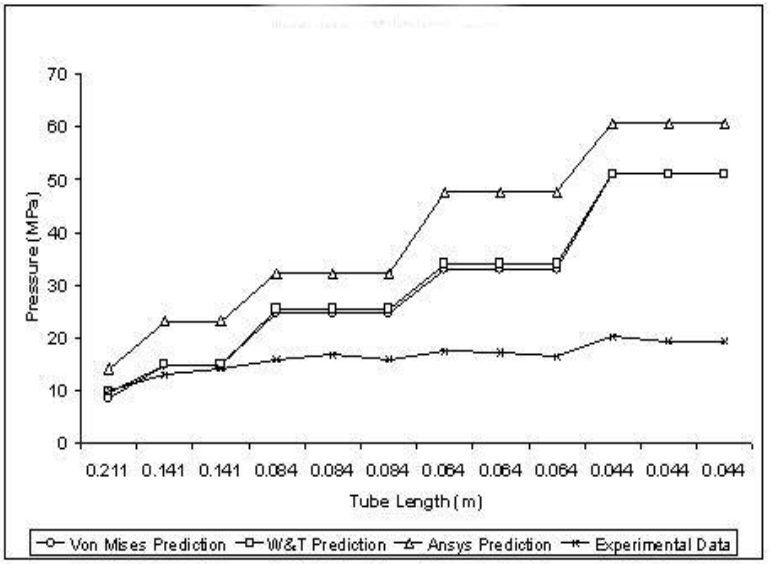

Figure 24: Graph of Predicted Buckling Pressures against tube lengths.

5. EVALUATION

It was apparent from studying the buckling pressures obtained from the theoretical and experimental results that the length and initial out-of-circularity of the tubes had a marked influence on the buckling resistance, particularly for the shorter tubes. The experimental study showed that stresses due to manufacturing should be considered in establishing the ultimate buckling resistance, in addition to the pipe thickness, diameter, length and ovality.

6. CONCLUSIONS

The experimental and theoretical investigations were performed successfully on all test samples, with the exception of the 50 and 30mm lengths because their experimental buckling pressures would have exceeded the maximum permitted design pressure of the tank.

- All specimens tested failed by shell instability.
- All specimens suffered from manufacturing imperfections. They were not concentric and precise diametric measurements clearly showed variations in tube wall thickness.
- Initial imperfections of the aluminium alloy tubes of the present paper were between 0.104t to 0.13t, where 't' was the wall thickness of the vessels, and the corresponding values for those of Windenburg and Trilling were between 0.11t and 0.16t, where 't' was the wall thickness of their vessels.
- Failures occurred in the areas of thinner wall thickness, due, it is thought to higher stress concentrations at these points; this was predicted by Mechanica.
- The analyses carried out with the three methods resulted in small differences between the theoretical buckling pressures.
- Theoretical buckling pressures were far higher than the actual buckling pressures recorded during pressure testing, especially for shorter vessels; this was due to initial values of out-of-circularity.
- The paper shows that the design charts appear to be suitable for designing such vessels; although there may be some scale effect.
- The design charts should only be applied to circular cylinders under uniform external pressure and whose initial out-of-circularity does not exceed 0.16t, where 't' is the wall thickness of such vessels.
- The plastic buckling method of using ANSYS via the Pro Engineer/Mechanica route, as described here is not practical for the design of large vessels, such as submarine pressure hulls, as their metrological data during design is required prior to manufacture, which is impossible.
- The detrimental effects of initial built-in stresses due to manufacture have not been taken into account.

REFERENCES

[1] R. von Mises, "Der Kritische Aussendruck für Allseits Belastete Zylindrische Rohre", Fest Zum 70. Geburtstag von Prof. Dr. A. Stodola, Zürich, pp. 418-30. Translated and annotated by D.F. Windenburg, 1936, Report No. 366, DTMB, Washington D.C, USA, 1929.

[2] D.F. Windenburg and C. Trilling, "Collapse by Instability of Thin Cylindrical Shells Under External Pressure", Trans., ASME, 11, pp 819-825, 1934.

[3] C.T.F. Ross, "Pressure Vessels: External Pressure Technology." Horwood Publishing Ltd., Chichester, UK, 2001. (http://www.mech.port.ac.uk/sdalby/mbm/CTFRProg2.htm)

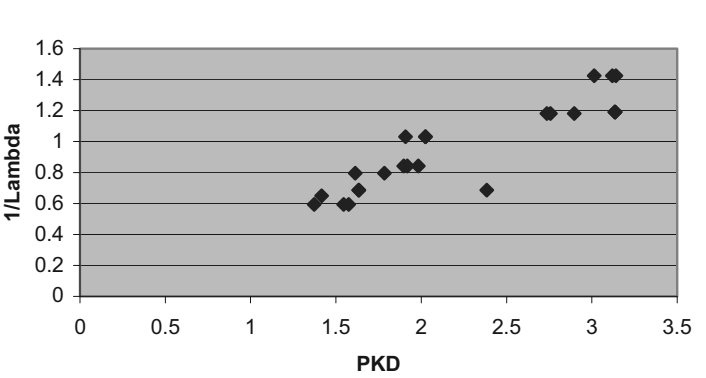

Figure 25: ANSYS Shell 93 for 2006 & 2007 results.

[4] T. Tokugawa, "Model Experiments on the Elastic Stability of Closed and Cross-Stiffened Circular Cylinders under Uniform External Pressure", Proc. World Engineering Congress, Tokyo, Vol.29, Paper No.651, pp.249-79, 1929.

[5] S. Kendrick, "The Buckling under External Pressure of Circular Cylindrical Shells with Evenly Spaced Equal Strength Circular Ring Frames –Part 1", NCRE Report No. R.211, 1953.

[6] C. T. F. Ross, "Mechanics of Solids", Horwood Publishing Ltd., Chichester, UK, 1999.

.

[7] T. E. Reynolds, "Inelastic Lobar Buckling of Cylindrical Shells under External Hydrostatic Pressure", DTMB Report No. 1392, Aug., 1960.

[8] T.G.Bosman, N.G. Pegg & P.J. Kenning, "Experimental and Numerical Determination of Non-Linear Overall Collapse of Imperfect Pressure Full Compartments", Int. Symp on Naval Submarines 4, RINA, 11-13 May, 1993,London.

[9] A. Nagoppan, "Buckling of Aluminium Alloy tubes under external water pressure." Mechanical Engineering Student Project Report, University of Portsmouth, Portsmouth, UK, June 2006.

